Shielding of Wire Segments and Loops in Electric Circuits by Spherical Shells

DIRK QUAK AND ADRIANUS T. DE HOOP

Abstract—**The susceptibility of an electric circuit to electromagnetic radiation incident on it is analyzed by the application of Lorentz's reciprocity relation. An equivalent Thevenin or Norton representation of the circuit serves to determine the induced signals quantitatively. The effect of a (multilayered) spherical shield on the performance of elementary parts of the circuit, viz., a short wire segment and a loop placed at the center of the shield, is investigated. The corresponding shielding performance is expressed as the reduction of the induced source strength in the equivalent networks. Numerical results are presented in a frequency range that includes the occurrence of internal resonances in the shielding structure.**

I. Introduction

IN THE ANALYSIS of the electromagnetic compatibility of electric circuits, one of the interferences to be investigated is the interaction between such a circuit and electromagnetic radiation incident on it from sources located elsewhere. Should the degradation of the performance of the circuit exceed the prescribed immunity level, shielding measures have to be taken.

In the present paper, we first analyze the susceptibility of an electric circuit to electromagnetic radiation incident on it by a proper application of Lorentz's reciprocity relation. An arbitrary N-port (for example, a nonshielded part of the circuit) is separated from the rest of it, the remainder being regarded as the load of the N-port (a shielded part, for example). It is shown that the amount of degradation of this system can be deduced from its equivalent active N-port network that can be either of the Thevenin (induced voltage source) or the Norton (induced current source) type, the accessible ports of which are terminated by the load. The entire system is assumed to be linear and time-invariant in its electromagnetic behavior, while all fields are assumed to be causally related to their sources. In view of this property, the analysis is carried out in the complex frequency or s-domain (s is the time Laplace transform parameter).

With the aid of the theory, the effect of shielding to incident radiation is investigated quantitatively. In particular, we determine exactly the influence of a multilayered spherical shield on the performance of the elementary parts in an electric circuit, viz., a short wire segment and a loop placed at the center of the shield, each of the layers of which has its own conductivity, permittivity, and permeability. Our paper is somewhat complementary to the usual literature on the subject, where the influence of shields is mostly expressed by an equivalent decrease of the incident electromagnetic field at some point [1]–[3]. Through the use of the reciprocity theorem, we directly express the influences of the shield in terms of the source strengths in the equivalent active circuit. The equivalence of the two concepts is the basis of the property that the shielding behavior of an enclosure can be determined not only by direct measurement or calculation of the interior fields but also by the transmitting properties of an internal source. The relevant concept has been previously utilized in EMC and EMI test programs as a "sniff" test, in which a small transmitter is positioned at various locations within the enclosure, and its external electromagnetic field is measured.[1] The analysis presented by Michielsen [4] is, in its point of view, similar to ours; it deviates, however, in the application of the theory to specific shielding structures. The paper extends earlier work by Schelkunoff [5] on spherical shielding structures to the higher frequency range at which his approximations (that either the shield thickness is large compared to the skin depth or the radius of the shield is small compared to the wavelength, or both) no longer hold.

Manuscript received July 12, 1988; revised January 1989.

The authors are with the Department of Electrical Engineering, Laboratory of Electromagnetic Research, Delft University of Technology, Delft, The Netherlands.

IEEE Log Number 8928161.

II. The Field Problem and Its Equivalent Network

For the positioning in space, an orthogonal Cartesian reference frame with origin 0 and three mutually perpendicular base vectors $\{\underline{i}_x, \underline{i}_y, \underline{i}_z\}$ of unit length each forming in the indicated order a right-handed system, is introduced. The position vector is denoted by $\underline{r} = x\underline{i}_x + y\underline{i}_y + z\underline{i}_z$ and the time coordinate by t. We present the analysis in the complex frequency or s-domain, where s is the time Laplace-transform parameter. The causality condition requires that all s-domain quantities are regular for complex s in some right halfplane $Re(s) > s_0$. The complex steady-state representation of sinusoidally oscillating fields of angular frequency ω follows upon taking $s = j\omega$. This corresponds to the complex exponential time dependence $\exp(j\omega t)$.

The electromagnetic properties of the media are characterized in the s-domain by the conductivity tensor $\underline{\underline{\sigma}}$, the permittivity tensor $\underline{\underline{\epsilon}}$, and the permeability tensor $\underline{\underline{\mu}}$, which may vary with position and depend on s. The representation of the constitutive parameters by symmetrical tensors of rank two indicates that anisotropy of the media is taken into account, a feature that is called for if modern integrated circuits are to be incorporated in the analysis. For an isotropic medium, the constitutive parameters reduce to scalars. To simplify the

[1] For this remark on EMC tests, the authors are indebted to one of the reviewers.

notation, we introduce the tensorial specific transverse admittance

$$\underline{\underline{\eta}} = \underline{\underline{\sigma}} + s\underline{\underline{\epsilon}} \tag{1}$$

and the tensorial specific longitudinal impedance

$$\underline{\underline{\zeta}} = s\underline{\underline{\mu}} \tag{2}$$

of the media. The s-domain electromagnetic field equations are then given by

$$-\underline{\nabla}\times\underline{H} + \underline{\underline{\eta}} \cdot \underline{E} = -\underline{J} \tag{3}$$

and

$$\underline{\nabla}\times\underline{E} + \underline{\underline{\zeta}} \cdot \underline{H} = -\underline{K}. \tag{4}$$

Here, $\underline{E}$ denotes the electric field strength, $\underline{H}$ the magnetic field strength, $\underline{J}$ the volume source density of electric current, and $\underline{K}$ the volume source density of magnetic current, all in the s-domain.

The starting point of our analysis is Lorentz's reciprocity theorem for a bounded domain D (Appendix A). Further, the theory is developed along the lines that are in use analyzing, in telecommunication engineering, the transmitting and receiving properties of radiating systems (such as antennas) terminating in networks [6]–[7]. For our case, let the reciprocity theorem be applied to the domain D that is bounded externally by the closed surface S^i across which electromagnetic radiation is incident on the susceptible system and bounded internally by a surface S^L across which the N-port is connected to the load (Fig. 1). Typically, at S^i, the field description is necessary, while at S_L, the port description with voltages and currents applies (Appendix B). On S^i, field measurements can be carried out. In between S^i and S^L, no external sources are assumed to be present, and hence, upon taking the media in states R and T (cf. (B.7) and (B.8)) to be the same, the relation

$$\int_{S^i} \underline{\nu} \cdot (\underline{E}^R\times\underline{H}^T - \underline{E}^T\times\underline{H}^R)\, dA = \sum_{\alpha=1}^{N} (-V_\alpha^R I_\alpha^T + V_\alpha^T I_\alpha^R) \tag{5}$$

holds. In (5), the superscript T denotes the state in which the system is in the transmitting situation (all sources of electromagnetic fields are contained within S^L), and the superscript R denotes the receiving situation (all sources of electromagnetic fields are located outside S^i). V_α is the voltage across the α-th port and I_α the current flowing through the α-th port into the load.

In the transmitting situation, let the accessible ports be excited by feeding the currents I_β^T ($\beta = 1, \cdots, N$) into them. In view of the linearity of the system, the voltages V_α^T ($\alpha = 1, \cdots, N$) across the ports are linearly related to the currents via either

$$V_\alpha^T = -\sum_{\beta=1}^{N} Z_{\alpha,\beta} I_\beta^T, \qquad (\alpha = 1, \cdots, N) \tag{6}$$

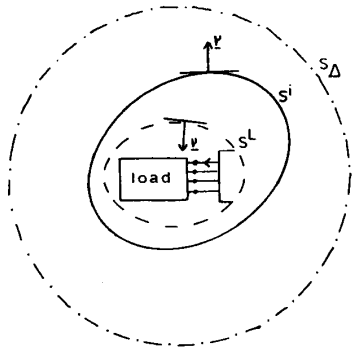

Fig. 1. Electromagnetic multiport system as a receiving system susceptable to electromagnetic radiation incident across S^i. On S^i, the field description is used; on S^L, the local port description applies. S_Δ is the sphere with radius Δ and center at the origin.

where $[Z]$ is the input impedance matrix, or

$$I_\alpha^T = -\sum_{\beta=1}^{N} Y_{\alpha,\beta} V_\beta^T, \qquad (\alpha = 1, \cdots, N) \tag{7}$$

where $[Z]$ is the input admittance matrix of the transmitting N-port system. These matrices are symmetric and are each other's inverse. Note that the transmitting situation applies to the actual configuration so that $[Z]$ and $[Y]$ depend on the positioning and shielding properties of the shields.

Next, we consider the electromagnetic N-port system as a receiving system, susceptible to incident radiation. In general, the accessible terminals are then connected to an N-port load (Fig. 1). To relate the receiving situation to the transmitting one, the total field in it is written as the sum of the incident field $\{\underline{E}^i, \underline{H}^i\}$ that is emitted by the sources outside S^i and that would be the total field if the load were "absent" and the scattered field $\{\underline{E}^s, \underline{H}^s\}$ that is the field that must be superimposed on the incident field to yield the total field in the presence of the load. Correspondingly, we have

$$\{\underline{E}^R, \underline{H}^R\} = \{\underline{E}^i + \underline{E}^s, \underline{H}^i + \underline{H}^s\}. \tag{8}$$

(What "absence" of the load actually implies for the description of the receiving system will be elucidated further on.) From (5), we then obtain

$$\int_{S^i} \underline{\nu} \cdot [(\underline{E}^i + \underline{E}^s)\times\underline{H}^T - \underline{E}^T\times(\underline{H}^i + \underline{H}^s)]\, dA = \sum_{\alpha=1}^{N} (-V_\alpha^R I_\alpha^T + V_\alpha^T I_\alpha^R). \tag{9}$$

Now, both $\{\underline{E}^s, \underline{H}^s\}$ and $\{\underline{E}^T, \underline{H}^T\}$ are source-free in the domain exterior to S^i, and both are causally related to the action of sources located in the bounded domain interior to S^i. Consequently,

$$-\int_{S^i} \underline{\nu} \cdot (\underline{E}^s\times\underline{H}^T - \underline{E}^T\times\underline{H}^s)\, dA = \int_{S_\Delta} \underline{\nu} \cdot (\underline{E}^s\times\underline{H}^T - \underline{E}^T\times\underline{H}^s)\, dA \tag{10}$$

where S_Δ is a sphere with radius Δ and center at the origin of the chosen coordinate system that completely surrounds S^i. In the limit $\Delta \to \infty$, however, the right-hand side of (10) vanishes. Now, the left-hand side of (10) is independent of Δ, and therefore

$$\int_{S^i} \underline{v} \cdot (\underline{E}^s \times \underline{H}^T - \underline{E}^T \times \underline{H}^s)\, dA = 0. \tag{11}$$

Using (11) in (9), we obtain

$$\int_{S^i} \underline{v} \cdot (\underline{E}^i \times \underline{H}^T - \underline{E}^T \times \underline{H}^i)\, dA = \sum_{\alpha=1}^{N} (-V_\alpha^R I_\alpha^T + V_\alpha^T I_\alpha^R). \tag{12}$$

Next, we express the dependence of $\underline{E}^T$ and $\underline{H}^T$ on the way in which the N accessible ports are fed by writing $\{\underline{E}^T, \underline{H}^T\} = \Sigma_{\alpha=1}^N \{\underline{e}'_\alpha, \underline{h}'_A\} I_\alpha^T$. By using this and (6) in (12), we arrive at the Thevenin representation

$$V_\alpha^e = V_\alpha^R + \sum_{\beta=1}^{N} Z_{\alpha,\beta} I_\beta^R, \qquad (\alpha = 1, \cdots, N) \tag{13}$$

in which

$$V_\alpha^e = -\int_{S^i} \underline{v} \cdot (\underline{E}^i \times \underline{h}'_\alpha - \underline{e}'_\alpha \times \underline{H}^i)\, dA, \qquad (\alpha = 1, \cdots, N). \tag{14}$$

Equation (13) is representative for an N-port network with internal voltage sources V_α^e ($\alpha = 1, \cdots, N$) and an internal impedance matrix that is the symmetric input impedance matrix of the same N-port in the transmitting situation. As (13) shows, "absence" of the load in this description means that the loaded terminals of the N-port are left open, i.e., $I_\beta^R = 0$ for all β, and hence, $V_\alpha^R = V_\alpha^e$ for all α.

In the same way, we can express that $\{\underline{E}^T, \underline{H}^T\}$ are linearly related to the values of the voltages $\{V_\alpha^T\}$ by writing $\{\underline{E}^T, \underline{H}^T\} = \Sigma_{\alpha=1}^N \{\underline{e}''_\alpha, \underline{h}''_\alpha\} V_\alpha^T$. By using this and (7) in (12), we arrive at the Norton representation

$$I_\alpha^e = \sum_{\beta=1}^{N} Y_{\alpha,\beta} V_\beta^R + I_\alpha^R, \qquad (\alpha = 1, \cdots, N) \tag{15}$$

in which

$$I_\alpha^e = \int_{S^i} \underline{v} \cdot (\underline{E}^i \times \underline{h}''_\alpha - \underline{e}''_\alpha \times \underline{H}^i)\, dA, \qquad (\alpha = 1, \cdots, N). \tag{16}$$

Equation (16) is representative for an N-port network with internal current sources I_α^e ($\alpha = 1, \cdots, N$) and an internal admittance matrix that is the symmetric input admittance matrix of the same N-port in the transmitting situation. As (15) shows, "absence" of the load in this description means that the loaded terminals of the N-port are short-circuited, i.e., $V_\beta^R = 0$ for all β, and hence, $I_\alpha^R = I_\alpha^e$ for all α.

For a one-port system, the Thevenin and the Norton representations are shown in Fig. 2.

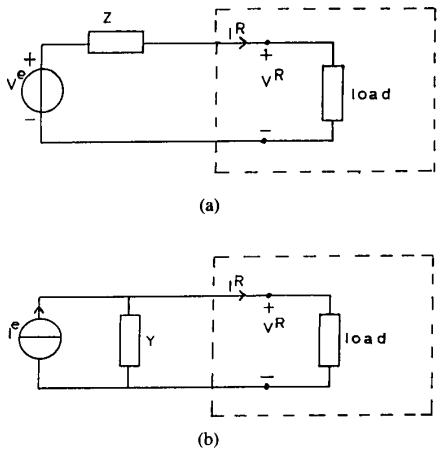

Fig. 2. (a) Thevenin representation and (b) Norton representation of an electromagnetic one-port system in the receiving situation.

III. The Influence of Spherical Shields on the Susceptibility of Wire Segments and Wire Loops Placed in Its Center

To analyze the influence of a shielding structure, one can adopt two points of view. The first, and most common, is that S^i is taken interior to the shielding structure, which implies that in the right-hand sides of (14) or (16), the values of $\{\underline{E}^i, \underline{H}^i\}$ change (and hopefully reduce), while the values of $\{\underline{e}'_\alpha, \underline{h}'_\alpha\}$ or $\{\underline{e}''_\alpha, \underline{h}''_\alpha\}$, respectively, remain the same. The second is that S^i is taken exterior to the shielding structure, which implies that in the right-hand sides of (14) or (16), the values of $\{\underline{E}^i, \underline{H}^i\}$ remain the same, while the values of $\{\underline{e}'_\alpha, \underline{h}'_\alpha\}$ or $\{\underline{e}''_\alpha, \underline{h}''_\alpha\}$, respectively, change (and hopefully reduce). This equivalence is the basis of the "sniff" test mentioned in the Introduction. As will be illustrated below, $\{\underline{E}^T, \underline{H}^T\}$ and thus the related $\{\underline{e}'_\alpha, \underline{h}'_\alpha\}$ or $\{\underline{e}''_\alpha, \underline{h}''_\alpha\}$, are in many cases much easier to calculate (they are only related to the circuit under investigation) than $\{\underline{E}^i, \underline{H}^i\}$, since the latter are related to, in many cases unknown, sources located elsewhere. This is why we base our analysis on the latter point of view.

One of the shielding problems that can be solved by rather elementary means (and has also been considered by Schelkunoff [5]) is the one pertaining to multilayered spherical shields with a short wire segment or a small loop placed at its center in case this whole structure is embedded in a homogeneous, isotropic medium. In view of (14) or (16), we then need the fields $\{\underline{E}^T, \underline{H}^T\}$ transmitted by such a wire segment or a loop, carrying a uniform current I^T. Let σ, ϵ, and μ be the scalar conductivity, permittivity, and permeability, respectively, of the embedding medium; then, $\{\underline{E}^T, \underline{H}^T\}$ are, in general, given by

$$\underline{E}^T = -\zeta \underline{A} + \eta^{-1} \underline{\nabla}(\underline{\nabla} \cdot \underline{A}) - \underline{\nabla} \times \underline{F} \tag{17}$$

and

$$\underline{H}^T = -\eta \underline{F} + \zeta^{-1} \underline{\nabla}(\underline{\nabla} \cdot \underline{F}) + \underline{\nabla} \times \underline{A} \tag{18}$$

where $\{\underline{A}, \underline{F}\}$ are the vector potentials of the source distributions of the transmitting system.

For a short, straight segment of conducting wire of vectorial length $\underline{L}$ carrying the uniform current I^T placed at the center of the coordinate system and radiating into the infinite medium, we have

$$\underline{A} = I^T \underline{L} \exp(-\gamma|\underline{r}|)/4\pi|\underline{r}| \qquad \underline{F} = \underline{0} \tag{19}$$

where $\gamma = (\eta\zeta)^{1/2}$ with $Re(\gamma) > 0$ when $Re(s) > 0$ is the medium's propagation coefficient, and $\underline{r}$ denotes the point of observation.

To analyze the shielding efficiency of a spherical shield around this transmitter, we can write $\underline{A} = I^T \underline{L} U$. In the absence of the shield, $\underline{A}$ depends on $\underline{r}$ only through the omnidirectional scalar spherical wave function U, which corresponds to a wave diverging from the center $\underline{r} = \underline{0}$ and satisfies the modified Helmholtz equation $\underline{\nabla} \cdot \underline{\nabla} U - \gamma^2 U = -\delta(\underline{r})$, where $\delta(\underline{r})$ is the three-dimensional unit impulse acting at $\underline{r} = \underline{0}$. It is now anticipated that in the presence of the shield, the directional structure of $\underline{A}$ remains the same, while only the radial one changes due to successive reflections and transmissions in the layers. In the ball interior to the shield, an omnidirectional standing wave that is bounded at $\underline{r} = \underline{0}$ is superimposed upon the wave diverging from the source. In the spherical shells, the wave field is a superposition of omnidirectional diverging and converging waves. In the domain outside the shield, the wave function remains a diverging omnidirectional spherical wave albeit with a different amplitude. All these spherical waves are solutions to the radial transmission-line equations and show pertinent corresponding radial spherical wave impedances.

The configuration that we consider consists of a domain D_1, for which $0 < |\underline{r}| < r_1$, interior to the shield (i.e., the domain where the radiating element is situated), the shielding domain consisting of $(ND - 2)$ different concentric, spherical shells D_M, for which $r_{M-1} < |\underline{r}| < r_M (M = 2, \cdots, ND - 1)$, and the domain D_{ND}, for which $r_{ND-1} < |\underline{r}| < \infty$, exterior to the shield (Fig. 3). The total number of domains in the configuration is ND. In each subdomain D_M a homogeneous, isotropic medium is present with transverse admittance per length $\eta_M = \sigma_M + s\epsilon_M$ and longitudinal impedance per length $\zeta_M = s\mu_M$, while the propagation coefficient is $\gamma_M = (\eta_M \zeta_M)^{1/2}$ with $Re(\gamma_M) > 0$ if $Re(s) > 0$. The representation of the scalar wave function $U = U(|\underline{r}|)$ in the domain D_M is written as

$$U_M = U_M^+ \frac{\exp[-\gamma_M(|\underline{r}| - r_{M-1})]}{4\pi|\underline{r}|} + U_M^- \frac{\exp[-\gamma_M(r_M - |\underline{r}|)]}{4\pi|\underline{r}|}$$

$$\text{when } r_{M-1} < |\underline{r}| < r_M, \qquad (M = 1, \cdots, ND). \tag{20}$$

In (20), U_M^+ and U_M^- are constant coefficients. Each term on the right-hand side of (20) satisfies the source-free modified Helmholtz equation as long as $|\underline{r}| \neq 0$. The constant parts in the arguments of the exponential functions have been included to avoid the loss of significant figures in the numerical handling of the expressions in case γ_M gets large. In D_1, the wave function that must be superimposed on the diverging one

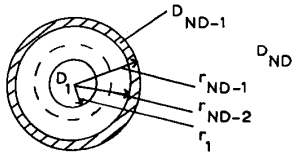

Fig. 3. Spherical configuration, consisting of $(ND - 2)$ shells D_M for which $r_{M-1} < |\underline{r}| < r_M$ with $M = 2, \cdots, ND - 1$.

to account for the presence of the shield must be bounded at $|\underline{r}| = 0$. This is accomplished by taking

$$U_1 = \frac{\exp(-\gamma_1|\underline{r}|)}{4\pi|\underline{r}|} + 2R \exp(-\gamma_1 r_1) \frac{\sinh(\gamma_1|\underline{r}|)}{4\pi|\underline{r}|}$$

$$\text{when } 0 < |\underline{r}| < r_1 \tag{21}$$

so $U_1^+ = 1 - R \exp(-\gamma_1 r_1)$ and $U_1^- = R$. In D_{ND}, the wave function must remain bounded as $|\underline{r}| \to \infty$, and hence, the term containing $\exp(\gamma_{ND}|\underline{r}|)/4\pi|\underline{r}|$ must be missing. Accordingly, we take

$$U_{ND} = T \frac{\exp[-\gamma_{ND}(|\underline{r}| - r_{ND-1})]}{4\pi|\underline{r}|}$$

$$\text{when } r_{ND-1} < |\underline{r}| < \infty \tag{22}$$

so $U_{ND}^+ = T$, and $U_{ND}^- = 0$. Note that (20)–(22) describe the shielding problem as a reflection, transmission, and attenuation process in which R is the overall reflection coefficient in the interior domain, T the overall transmission coefficient in the exterior domain, and the exponential functions in (20) describe the attenuation that takes place in the interior of the shells. The relationships between the coefficients $\{U_M^-, U_M^+\}$ with $M = 1, \cdots, ND$ follow from the boundary conditions at the interfaces $|\underline{r}| = r_M$ with $M = 1, \cdots, ND - 1$, which require the continuity of the tangential components of the electric and magnetic field strengths. Using (19) in (17)–(18), the field strengths for the radiating wire segment are found as

$$\underline{E}^T = (-\zeta U + \eta^{-1}|\underline{r}|^{-1}\partial_{|\underline{r}|} U) I^T \underline{L} + \eta^{-1}(-|\underline{r}|^{-1}\partial_{|\underline{r}|} U + \partial_{|\underline{r}|}\partial_{|\underline{r}|} U)\underline{\xi}(\underline{\xi} \cdot I^T \underline{L}) \tag{23}$$

and

$$\underline{H}^T = \underline{\xi} \times I^T \underline{L} \partial_{|\underline{r}|} U \tag{24}$$

where $\underline{\xi} = \underline{r}/|\underline{r}|$ is the unit vector in the radial direction. We observe that the second term on the right-hand side of (23) points along $\underline{\xi}$; i.e., it has no component tangential to the interfaces. Therefore, the tangential components of the electric and magnetic field strengths are made continuous across an interface if we make $-\zeta U + \eta^{-1}|\underline{r}|^{-1}\partial_{|\underline{r}|} U$ and $\partial_{|\underline{r}|} U$ continuous across that interface. The relationships between $\{U_M^-, U_M^+, U_{M+1}^-, U_{M+1}^+\}$, with $M = 1, \cdots, ND - 1$, can be grouped together in the form of a scattering matrix denoted by $[S]_{M,M+1}$ and defined by

$$\begin{bmatrix} U_{M+1}^+ \\ U_M^- \end{bmatrix} = [S]_{M,M+1} \begin{bmatrix} U_{M+1}^- \\ U_M^+ \end{bmatrix}. \tag{25}$$

In the scattering matrices, the reflection and transmission

coefficients for radial spherical waves at each interface occur. The relevant expressions are somewhat lengthy and will not be given here.

For the multilayered shield, the overall scattering matrix $[S]_{1,ND}$ can formally be written as

$$[S]_{1,ND} = [S]_{1,2} * [S]_{2,3} * \cdots * [S]_{ND-2,ND-1} * [S]_{ND-1,ND} \quad (26)$$

in which * denotes the so-called Redheffer star product of matrices that has been introduced in [8]. From (25) and (26), we obtain

$$\begin{bmatrix} T \\ R \end{bmatrix} = [S]_{1,ND} \begin{bmatrix} 0 \\ 1 - R \exp(-\gamma_1 r_1) \end{bmatrix}. \quad (27)$$

To characterize the overall performance of the shield, the shielding effectiveness S is introduced, which is the ratio of the field strength at a point before and after the placement of the shield. The insertion of a shield around a circuit entails that the relation $\gamma_1 = \gamma_{ND}$ holds. So, for any point $|\underline{r}| > r_{ND-1}$, we have (cf. (22))

$$S = T^{-1} \exp(-\gamma_{ND} r_{ND-1}). \quad (28)$$

From (13)–(16), it is evident that the induced source strengths in the Thevenin or Norton representation of the susceptible circuit are modified by the shielding by the same factor S.

For a small loop with vectorial area $\underline{AR}$ carrying the uniform current I^T placed at the origin of the coordinate system and radiating into the infinite medium, we have

$$\underline{A} = \underline{0} \qquad \underline{F} = \zeta I^T \underline{AR} \exp(-\gamma|\underline{r}|)/4\pi|\underline{r}| \quad (29)$$

where $\underline{r}$ denotes the point of observation. The analysis of the shielding efficiency of a spherical shield with the loop at its center runs along the same lines as the one for the wire segment. We write $\underline{F} = \zeta I^T \underline{AR}\ V$, where V replaces the function U in the analysis of the wire segment. Using (29) in (17)–(18), the field strengths for the radiating loop are found as

$$\underline{E}^T = -\underline{\xi} \times \zeta I^T \underline{AR} \partial_{|\underline{r}|} V \quad (30)$$

and

$$\underline{H}^T = (-\eta V + \zeta^{-1}|\underline{r}|^{-1}\partial_{|\underline{r}|} V)\zeta I^T \underline{AR} + \zeta^{-1}(-|\underline{r}|^{-1}\partial_{|\underline{r}|} V + \partial_{|\underline{r}|}\partial_{|\underline{r}|} V)\underline{\xi}(\underline{\xi} \cdot \zeta I^T \underline{AR}). \quad (31)$$

In (31), the second term on the right-hand side points along $\underline{\xi}$, i.e., it has no component tangential to the interfaces. Therefore, the tangential components of the electric and magnetic field strength for the radiating loop are made continuous across an interface if we make $\zeta \partial_{|\underline{r}|} V$ and $-\zeta\eta V + |\underline{r}|^{-1}\partial_{|\underline{r}|} V$ continuous across that interface. Again, the coefficients that define V in the shells can be grouped in a matrix form as (25).

IV. Numerical Results and Conclusion

On the basis of the analysis in the previous sections, a computer program has been written that yields the shielding effectivenesses for a configuration consisting of a wire segment or a loop with a spherical shield around it. The shield may be multilayered; each layer may be composed of any kind of linear, isotropic material. When the calculations are performed on the basis of the scattering matrix formalism, they proceed without difficulty in the frequency regions in which we are interested and which are shown in the figures.

In Figs. 4, 5, and 6, the effect of a single shield around a wire segment or a loop is shown. In the frequency range used, two effects intermingle, i.e., the shielding effect of the conducting shield in its dependence on the ratio (skin depth)/(free-space wavelength) and the effect of resonances in dependence on the ratio (shield-radius)/(free-space wavelength). In Fig. 4, the shielding effectiveness of a conducting shield for a wire segment is presented as a function of normalized frequency r_1/λ, in which λ is the free-space wavelength. The shield consists of a single layer of copper ($\sigma = 5.65 * 10^7/\Omega\cdot$m) with thicknesses of $1 * 10^{-6}$ m, $3 * 10^{-6}$ m, and $5 * 10^{-6}$ m, respectively, whereas the inner radius of the shield is $5 * 10^{-2}$ m. From the figure, it is clear that the conducting shield forms an effective one for the wire segment. In the very-low-frequency region, the wire is perfectly shielded, even electrostatically. At the resonant frequencies of the spherical cavity, severe dips occur in the shielding effectiveness. In the low-frequency region, where $2\pi r_1/\lambda \ll 1$ holds, approximations to the wave impedances of the radial spherical waves and the radial spherical wave interface reflection and transmission coefficients can be made, after which the results reduce to the ones obtained by Schelkunoff [5]. In the figures, the frequency range considered exceeds the validity of these low-frequency approximations.

Fig. 5 shows that in accordance with that which has been found in [2], even near the resonant frequencies of the spherical structure, the shielding effectiveness is considerable, provided that the thickness of the shield exceeds the skin depth. When the quality factor of our numerically obtained resonance behavior for a shield thickness of several skin depths is compared with the one obtained by Schelkunoff [5] by equating the surface impedance of the sphere to the intrinsic impedance of a good conductor, they are in complete accordance.

In Fig. 6, the shielding effectiveness of the same configuration is presented, except now it is presented for a loop. The most significant difference with the shielding of the wire segment is the minimal shielding of a loop by a conducting shield at low frequencies. This is to be expected since, for the loop, the magnetic field is predominant at these frequencies, and this field penetrates across a conducting shield. The resonant frequencies for the loop differ from those for the wire segment.

For shields around a wire or a loop whose thickness is larger than several skin depths (in Figs. 4 and 6, curves (b) and (c), the mark in the curves indicates the point at which the skin depth equals the thickness of the shield), the position of the resonance frequencies of a spherical enclosure around the wire or the loop placed at its center and the exponential attenuation of the wave transversing it are in accordance with earlier investigations by Schelkunoff [5]. For the thinner shields

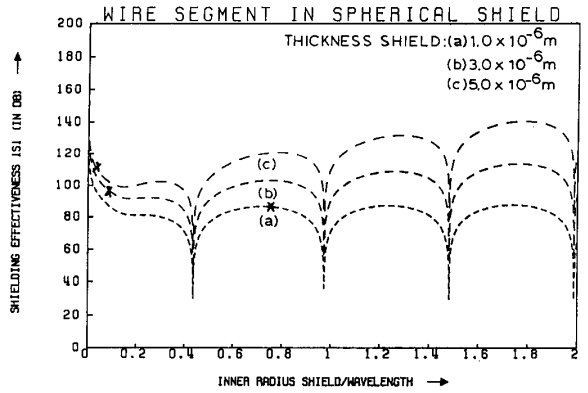

Fig. 4. Shielding effectiveness of a spherical shield for a wire segment at its center (copper shield placed in air (vacuum): inner radius shield = $5.0 * 10^{-2}$ m, conductivity shield = $5.65 * 10^{7}/\Omega \cdot$m). The mark indicates where the thickness of the shield equals the skin depth.

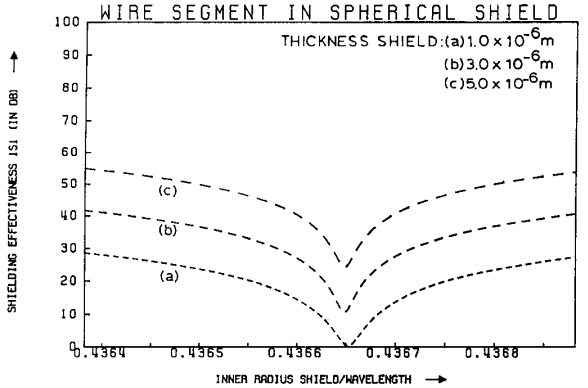

Fig. 5. Shielding effectiveness of a spherical shield for a wire segment at its center at the first resonance frequency (copper shield placed in air (vacuum): inner radius shield = $5.0 * 10^{-2}$ m, conductivity shield = $5.65 * 10^{7}/\Omega \cdot$m).

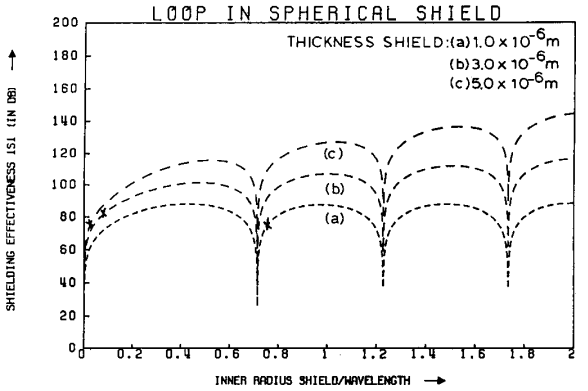

Fig. 6. Shielding effectiveness of a spherical shield for a loop at its center (copper shield placed in air (vacuum): inner radius shield = $5.0 * 10^{-2}$ m, conductivity shield = $5.65 * 10^{7}/\Omega \cdot$m). The mark indicates where the thickness of the shield equals the skin depth.

(Figs. 4 and 6, curve (a)), the increase of shielding effectiveness with frequency is much more modest, as is to be expected. In the entire frequency range shown in Figs. 4, 5, and 6, the condition for a "good conductor" applies to the

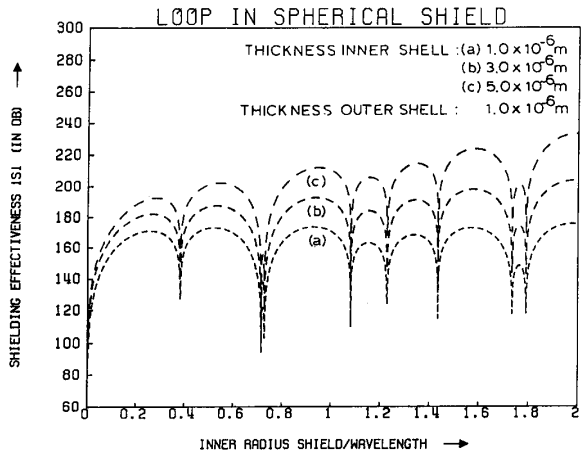

Fig. 7. Shielding effectiveness of a shield consisting of two separate concentric spherical shells for a loop at its center (copper shells placed in air (vacuum): inner radius inner shell = $5.0 * 10^{-2}$ m, inner radius outer shell = $12.0 * 10^{-2}$ m, conductivity of both shells = $5.65 * 10^{7}/\Omega \cdot$m).

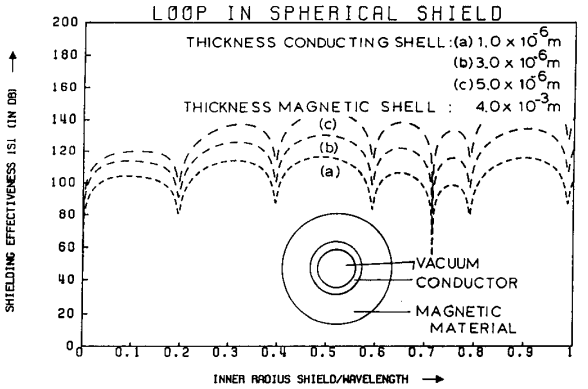

Fig. 8. Shielding effectiveness of a multilayered spherical shield with a loop at its center (conducting and magnetic shell placed in air (vacuum): inner radius conducting shell = $5.0 * 10^{-2}$ m, inner radius magnetic shell = outer radius copper shell, thickness magnetic shell = $4.0 * 10^{-3}$ m, conductivity copper shell = $5.65 * 10^{7}/\Omega \cdot$m, relative permeability magnetic shell = 1000).

shields, i.e., the electric displacement current is negligible with respect to the conduction current ($2\pi f\epsilon_0/\sigma$ is at most 10^{-8}).

The result of the application of two separate conducting shells around a loop is shown in Fig. 7. The overall shielding effectiveness increases, as expected, whereas the introduction of new resonant frequencies is the immediate consequence of the presence of the second shell with a different radius. Figs. 8 and 9 show the shielding effectiveness for a loop in a multilayered shield consisting of a conducting shell with thicknesses $1 * 10^{-6}$ m, $3 * 10^{-6}$ m, and $5 * 10^{-6}$ m, respectively and a magnetic shell with a thickness of $4 * 10^{-3}$ m. In Fig. 8, the conducting shell is located inside the magnetic shell, where as in Fig. 9, the magnetic shell is located inside the conducting shell. The shielding effectiveness of the combination in Fig. 9 is somewhat higher in the frequency range, where $2\pi r_1/\lambda \ll 1$ holds, than is the one in Fig. 8 (cf. [3]).

The use of the scattering matrix formalism leads in the very-

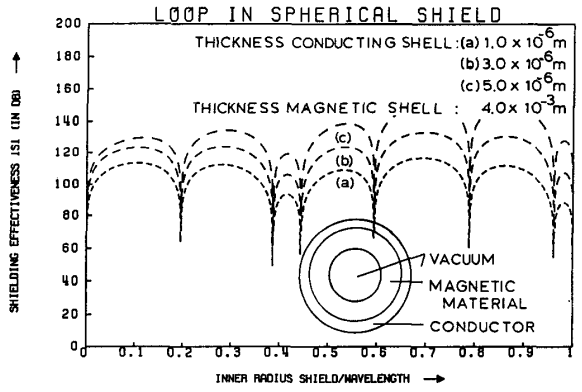

Fig. 9. Shielding effectiveness of a multilayered spherical shield with a loop at its center (magnetic and conducting shell placed in air (vacuum): inner radius magnetic shell = $5.0 * 10^{-2}$ m, inner radius conducting shell = 5.4 $* 10^{-2}$ m, relative permeability magnetic shell = 1000, conductivity copper shell = $5.65 * 10^{7}/\Omega \cdot$m).

low-frequency region to a loss in significant figures. In this region, an alternative representation for the wave functions is to be used that expresses their standing-wave behavior in the bounded subdomains, rather than the propagating wave description used in (20) and (25). Such a behavior is expressed via a relation of the type

$$U_M = U_M^c \frac{\cosh\left[\gamma_M(|\underline{r}| - r_{M-1})\right]}{4\pi|\underline{r}|} + U_M^s \frac{\sinh\left[\gamma_M(|\underline{r}| - r_{M-1})\right]}{4\pi|\underline{r}|}$$
$$\text{when } r_{M-1} < |\underline{r}| < r_M, \qquad (M = 1, \cdots, ND-1), \tag{32}$$

that replaces (20). In (32), U_M^c and U_M^s are constant coefficients. The relation between the coefficients in these representations follow again from the application of the pertaining boundary conditions. From the representations, (21), (22), and (32) again follow T and R and hence, follow with (28) the shielding effectiveness.

The paper illustrates the usefulness of the Lorentz's reciprocity relation as a starting point for analyzing shielding configurations as to their effectiveness. It puts the "sniff" test for EMC and EMI test programs on a rigorous mathematical basis. Further, it develops a numerically stable scheme that can handle, in a recursive manner, an arbitrary number of concentric spherical shells for an arbitrary frequency range. The results show, albeit for a specific model geometry, what type of behavior can be expected for the shielding effectiveness of laminated shields in dependence on their physical properties and dimensions.

Appendix A

The Reciprocity Theorem

We consider a time-invariant, bounded domain D in space in which two nonidentical electromagnetic states can occur. The two states will be distinguished by the superscripts T and R, respectively [9]. Neither the source distributions of the electromagnetic fields in the two states nor the media present in the two states need be the same. The boundary surface of D is denoted by ∂D; the unit vector $\underline{\upsilon}$ along the normal to ∂D is directed away from D. From (3) and (4), it follows immediately that the relation

$$\begin{aligned}\underline{\nabla} \cdot (\underline{E}^R \times \underline{H}^T - \underline{E}^T \times \underline{H}^R) &= \underline{H}^R \cdot (\underline{\underline{\zeta}}^T - \underline{\underline{\zeta}}^R) \cdot \underline{H}^T \\ &\quad - \underline{E}^R \cdot (\underline{\underline{\eta}}^T - \underline{\underline{\eta}}^R) \cdot \underline{E}^T - \underline{K}^R \cdot \underline{H}^T \\ &\quad - \underline{J}^T \cdot \underline{E}^R + \underline{K}^T \cdot \underline{H}^R + \underline{J}^R \cdot \underline{E}^T \end{aligned} \tag{A1}$$

holds. Equation (A1) is the local form of the Lorentz's reciprocity theorem. Integration of (A1) over the domain D and the use of Gauss' theorem in the resulting left-hand side lead to

$$\begin{aligned}\int_{\partial D} \underline{\upsilon} \cdot (\underline{E}^R \times \underline{H}^T - \underline{E}^T \times \underline{H}^R)\, dA &= \int_D [\underline{H}^R \cdot (\underline{\underline{\zeta}}^T - \underline{\underline{\zeta}}^R) \cdot \underline{H}^T - \underline{E}^R \cdot (\underline{\underline{\eta}}^T - \underline{\underline{\eta}}^R) \cdot \underline{E}^T]\, dV \\ &\quad + \int_D (\underline{J}^R \cdot \underline{E}^T - \underline{K}^R \cdot \underline{H}^T - \underline{J}^T \cdot \underline{E}^R + \underline{K}^T \cdot \underline{H}^R)\, dV. \end{aligned} \tag{A2}$$

Equation (A2) is Lorentz's reciprocity theorem in its global form for the domain D.

In case the reciprocity theorem has to be applied to an unbounded domain with nonvanishing sources in a bounded subdomain only, the case will be handled as the limiting case that occurs if D is taken to be the domain interior to a sphere S_Δ of radius Δ and center at the origin, and the limit $\Delta \to \infty$ is considered. The surface integral at the left-hand side of (A.2) that now has to be evaluated over S_Δ vanishes, since the field quantities occurring in the integrand show, due to causality, an exponential decay when $\mathrm{Re}(s) > 0$ and $|\underline{r}| \to \infty$.

Appendix B

The Interaction Over a Local Multiport System

In the neighborhood of local terminations, the electric field $\underline{E}$ can approximately be expressed in terms of a scalar potential $\Phi = \Phi(\underline{r}, s)$ through the relation

$$\underline{E} = -\underline{\nabla}\Phi. \tag{B1}$$

The terminals themselves are assumed to be perfectly conducting, which implies that on them, the scalar electric potential has a constant value. Let S^L denote a closed surface that surrounds the multiport system and thus excludes the domain of the multiport termination from the right-hand side of (A2). Then, we have (see Fig. 1)

$$\begin{aligned}\int_{S^L} \underline{\upsilon} \cdot (\underline{E}^R \times \underline{H}^T)\, dA &= -\int_{S^L} \underline{\upsilon} \cdot (\underline{\nabla}\Phi^R \times \underline{H}^T)\, dA \\ &= -\int_{S^L} \underline{\upsilon} \cdot \underline{\nabla} \times (\Phi^R \underline{H}^T)\, dA \\ &\quad + \int_{S^L} \Phi^R \underline{\upsilon} \cdot (\underline{\nabla} \times \underline{H}^T)\, dA. \end{aligned} \tag{B2}$$

However, on account of Stokes' theorem, we have

$$\int_{S^L} \underline{v} \cdot \underline{\nabla} \times (\Phi^R \underline{H}^T)\, dA = 0, \tag{B3}$$

since S^L is a closed surface, and $\Phi^R \underline{H}^T$ has been assumed to be continuous on S^L. Further,

$$\int_{S^L} \Phi^R \underline{v} \cdot (\underline{\nabla} \times \underline{H}^T)\, dA = \int_{S^L} \Phi^R \underline{v} \cdot \underline{\eta}^T \cdot \underline{E}^T\, dA. \tag{B4}$$

Now, in the local approximation, $\underline{\eta}^T \cdot \underline{E}^T$ on S^L is predominantly concentrated in the conduction current in the conductors joining the accessible ports with the remainder of the system. Let A_α be the cross-section of the α-th conductor ($\alpha = 1, \cdots, N$). Then

$$\int_{S^L} \Phi^R \underline{v} \cdot \underline{\eta}^T \cdot \underline{E}^T\, dA \approx \sum_{\alpha=1}^{N} \int_{A_\alpha} \Phi^R \underline{v} \cdot \underline{J}^T\, dA$$

$$= \sum_{\alpha=1}^{N} V_\alpha^R I_\alpha^T \tag{B5}$$

where V_α is the constant potential of the α-th conductor and

$$I_\alpha = \int_{A_\alpha} \underline{v} \cdot \underline{J}\, dA \tag{B6}$$

is the conduction current flowing through the α-th conductor into (note the orientation of v on S^L) the domain where the multiport transmitting system or load is located. In the local approximation, the left-hand side of (A2) therefore reduces to

$$\int_{S^L} \underline{v} \cdot (\underline{E}^R \times \underline{H}^T - \underline{E}^T \times \underline{H}^R)\, dA = \sum_{\alpha=1}^{N} (V_\alpha^R I_\alpha^T - V_\alpha^T I_\alpha^R). \tag{B7}$$

If in D no sources are present while the media in D in state T and in state R are the same reciprocal ones, it follows immediately from (A2) that the relation

$$\int_{S^i} \underline{v} \cdot (\underline{E}^R \times \underline{H}^T - \underline{E}^T \times \underline{H}^R)\, dA = -\int_{S^L} \underline{v} \cdot (\underline{E}^R \times \underline{H}^T - \underline{E}^T \times \underline{H}^R)\, dA \tag{B8}$$

holds. With (B7) and (B8), the connection between the field description on S^i and the local description in voltages and currents on S^L is made.

Acknowledgment

The authors wish to thank one of the anonymous reviewers who put their attention to the use of the "sniff" test in EMC and EMI test programs.

References

[1] C. W. Harrison, Jr. and C. H. Papas, "On the attenuation of transient fields by imperfectly conducting spherical shells," *IEEE Trans. Antennas Propagat*, vol. AP-13, no. 6, pp. 960-966, Nov. 1965.

[2] T. K. Wu and L. L. Tsai, "Shielding properties of thick conducting cylindrical shells," *IEEE Trans. Electromagn. Compat.*, vol. EMC-16, no. 4, pp. 201-204, Nov. 1974.

[3] G. Francheschetti, "Fundamentals of steady-state and transient electromagnetic fields in shielding enclosures," *IEEE Trans. Electromagn. Compat.*, vol. EMC-21, no. 4, pp. 335-348, Nov. 1979.

[4] B. L. Michielsen, "A new approach to electromagnetic shielding," in *Proc. Electromag. Compat. 1985, 6th Symp. and Tech. Exhibition,* Zurich, Switzerland, March 5-7, 1985, pp. 509-514.

[5] S. A. Schelkunoff, *Electromagnetic Waves*. New York: Van Nostrand, 1943, pp. 294-315.

[6] A. T. de Hoop, "The N-port receiving antenna and its equivalent electrical network," Philips Res. Repts., vol. 30, 1975, pp. 302-315 (Special issue in honor of C. J. Bouwkamp).

[7] R. E. Collin and F. J. Zucker, *Antenna Theory, Part 1*. New York: McGraw-Hill, 1969, p. 94.

[8] R. Redheffer, "Difference equations and functional equations in transmission-line theory," in *Modern Mathematics for the Engineer* (second series), E. F. Beckenbach, Ed. New York: McGraw-Hill, 1961.

[9] J. Van Bladel, *Electromagnetic Fields*. New York: McGraw-Hill, 1964, p. 193.